J Mol Model (2013) 19:5445–5456
DOI 10.1007/s00894-013-2023-5

ORIGINAL PAPER

Modeling the scavenging activity of ellagic acid and its methyl derivatives towards hydroxyl, methoxy, and nitrogen dioxide radicals

Manish Kumar Tiwari · Phool Chand Mishra

Received: 2 May 2013 / Accepted: 25 September 2013 / Published online: 8 November 2013

Abstract The reaction mechanisms involved in the scavenging of hydroxyl ($OH^{\cdot}$), methoxy ($OCH_3^{\cdot}$), and nitrogen dioxide ($NO_2^{\cdot}$) radicals by ellagic acid and its monomethyl and dimethyl derivatives were investigated using the transition state theory and density functional theory. The calculated Gibbs barrier energies associated with the abstraction of hydrogen from the hydroxyl groups of ellagic acid and its monomethyl and dimethyl derivatives by an OH· radical in aqueous media were all found to be negative. When $NO_2^{\cdot}$ was the radical involved in hydrogen abstraction, the Gibbs barrier energies were much larger than those calculated when the $OH^{\cdot}$ radical was involved. When $OCH_3^{\cdot}$ was the hydrogen-abstracting radical, the Gibbs barrier energies lay between those obtained with $OH^{\cdot}$ and $NO_2^{\cdot}$ radicals. Therefore, the scavenging efficiencies of ellagic acid and its monomethyl and dimethyl derivatives towards the three radicals decrease in the order $OH^{\cdot} >> OCH_3^{\cdot} > NO_2^{\cdot}$. Our calculated rate constants are broadly in agreement with those obtained experimentally for hydrogen abstraction reactions of ellagic acid with OH· and NO_2· radicals.

Keywords Ellagic acid · Antioxidant · Free radicals · Reaction mechanism · Application of density functional theory

Introduction

It is well established that certain free radicals known as reactive oxygen species (ROS) and reactive nitrogen oxide species (RNOS) react with biomolecules (e.g., nucleic acid bases, lipids, and proteins) and damage them [1–4]. In biological systems, these radicals can form through both enzymatic and nonenzymatic processes, and may be initiated by various factors, such as environmental pollution, excess consumption of packaged food, smoking, and stressful living [5–9]. An excess of free radicals in biological systems, as caused by an imbalance between radical formation and radical removal or modification, leads to oxidative or nitrative stress [4, 5]. The main ROS include the hydroxyl radical ($OH^{\cdot}$), the peroxyl radical ($OOR^{\cdot}$), the methoxy radical ($CH_3O^{\cdot}$), and the carbonate radical anion ($CO_3^{\cdot-}$) [10], while the main RNOS include $NO^{\cdot}$, $NO_2^{\cdot}$, and $ONOO^{-}$ (peroxynitrite). $OH^{\cdot}$ radicals can form due to homolytic fission of the O–O bond of H_2O_2 in the presence of ionizing radiation or certain metal cations, such as Fe^{++} or Cu^{+} (Fenton reaction) [11]. Methoxy radicals can be produced by the photolysis of methyl acetate, the pyrolysis of dimethyl peroxide, or the radiolysis of liquid methanol [12]. Peroxynitrite is both an ROS and an RNOS, as it can cause both oxidative and nitrative damage to biological systems [13–16]. The $NO_2^{\cdot}$ radical is produced through either the homolysis of the conjugate acid of peroxynitrite (ONOOH) to $OH^{\cdot}$ and $NO_2^{\cdot}$ radicals [17–19] or the dissociation of the nitrosoperoxycarbonate anion ($ONOOCO_2^{-}$), formed by the reaction of peroxynitrite and CO_2 [19]. ROS and RNOS react with DNA bases, producing several mutagenic products [19–28] that can cause mutations and various diseases such as cancer and cardiovascular, Alzheimer's, and Parkinson's diseases [1–4].

Certain chemical species called antioxidants are present in biological systems that scavenge ROS and RNOS by converting them into nonreactive forms. Among these endogenous antioxidants are both enzymes and nonenzymes, such as superoxide dismutase, melatonin, glutathione, and bilirubin [29, 30]. Antioxidants that may be obtained from external sources include ascorbic acid (vitamin C), α-tocopherol

Electronic supplementary material The online version of this article (doi:10.1007/s00894-013-2023-5) contains supplementary material, which is available to authorized users.

M. K. Tiwari · P. C. Mishra (✉)
Department of Physics, Banaras Hindu University,
Varanasi 221 005, India
e-mail: pcmishra_in@yahoo.com

(vitamin E), curcumin, β-carotene, and *N*-acetylcysteine [6, 31]. However, the concentrations of endogenous antioxidants may become inadequate to scavenge free radicals during disease states. In such a situation, the use of external antioxidants becomes very important [32]. Many natural antioxidants are obtained from plants [33]. For example, ellagic acid is a plant phenolic compound that can provide a significant part of our daily external antioxidant dose [34, 35]. Ellagic acid is obtained from ellagitannins, which are the main components of plant cell walls [35]. Ellagitannins contain high molecular weight proteins and alkaloids and are soluble in water. Ellagic acid is also found in berries, other fruits and different types of food items, such as strawberries, raspberries, cranberries, grapes, blackcurrants, walnuts, pecans, and distilled beverages [36–43]. The commonly occurring methyl derivatives of ellagic acid are 3′-*O*-methyl ellagic acid, 3,3′-di-*O*-methyl ellagic acid and 3′, 4′-di-*O*-methyl ellagic acid [44]. In previous studies, it has been shown that ellagic acid and its methyl derivatives possess anticarcinogenic [45, 46], antimutagenic, and anti-inflammatory properties [47]. It has been also shown that ellagic acid is a more efficient radical scavenger than vitamin C and vitamin E [48]. Using pulse radiolysis, it has been found that ellagic acid scavenges hydroxyl and nitrogen dioxide radicals very efficiently [49].

Different parts of the ellagic acid molecule play various biological roles. For example, its lactone groups are involved in reducing the formation of O^6-methylguanine by participating in reactions involving certain carcinogens [50], while its four hydroxyl groups reduce CYPlAl-dependent benzo[*a*]pyrene hydroxylase activity [50]. It has been shown that ellagic acid binds with DNA due to its planar geometry and stacks between the DNA helical stands at orientations of 66–90° with respect to the DNA helix axis [48]. Due to this binding, ellagic acid prevents the mutagenesis of DNA caused by carcinogens [48]. Ellagic acid and its methyl derivatives inhibit the toxin PLA_2, which occurs in a deadly snake poison [37]. Ellagic acid has also been used for blood clotting because it is a natural hemostatic agent [44]. Further, it has been found that ellagic acid acts as an antiglycating agent, and this means that it inhibits AGEs (advanced glycation end-products), thereby reducing the risk of diabetes [51].

Thus, ellagic acid and its methyl derivatives play several important roles in biological systems. In view of this, in the work reported in the present paper, we investigated the reaction mechanisms involved in the scavenging of hydroxyl ($OH^{\cdot}$), nitrogen dioxide ($NO_2^{\cdot}$), and methoxy radicals ($OCH_3^{\cdot}$) by ellagic acid and its three methyl derivatives using a reliable theoretical approach.

Computational details

The geometries of the three conformers of ellagic acid were optimized using the B3LYP and B3PW91 functionals of density functional theory (DFT) along with the 6-31G(d,p) basis set in the gas phase [52–58]. Subsequently, to study the relative stabilities of the three conformers of ellagic acid, single-point energy calculations were performed using the abovementioned two density functionals along with the AUG-cc-pVDZ basis set in the gas phase. Transition state theory was employed to study the reaction mechanisms involved in the scavenging of $OH^{\cdot}$, $NO_2^{\cdot}$, and $OCH_3^{\cdot}$ by ellagic acid and its three methyl derivatives [59]. The geometries of all reactant complexes (RCs), transition states (TSs), and product complexes (PCs) involving ellagic acid and its mono- and dimethyl derivatives were optimized at the B3LYP/6-31G(d,p) level of theory. This was followed by single-point energy calculations employing the B3LYP and B3PW91 functionals along with the AUG-cc-pVDZ basis set in the gas phase for all the RCs, TSs, and PCs. $<S^2>$ at all the optimized RCs, TSs, and PCs was found to be close to 0.75 (doublet multiplicity), so spin contamination was negligible. Vibrational frequency analyses were carried out and the necessary thermal energy corrections to the total energy made so as to obtain Gibbs barrier energies at 298.15 K in the gas phase. The validity of the transition states was ensured by performing a visual inspection of vibrational modes corresponding to the imaginary frequencies at the transition states. These vibrational motions connected the reactants and products convincingly, and intrinsic reaction coordinate (IRC) calculations were not needed in any case. The gas-phase optimized RCs, TSs, and PCs involved in the calculations were solvated in aqueous media at the level of single-point energy calculations employing the polarizable continuum model (PCM) [54, 55]. The thermal energy corrections obtained in the gas phase were also considered to be valid for aqueous media. Rate constants were calculated, employing transition state theory [59]. The Windows version of the Gaussian G09 suite of programs (G09W) was used for all of the calculations, while the GaussView 5.0 suite of programs was used to visualize the molecular structures and vibrational modes [60, 61].

Results and discussion

Conformational analysis and molecular geometry

The structures of ellagic acid and its three methyl derivatives are given in Fig. 1a. The atomic numbering scheme employed in the present work is shown in this figure. The optimized structures of three conformers of ellagic acid, denoted EA-1, EA-2, and EA-3, are shown in Fig. 1b, c, and d, respectively. In each of these three conformers, the two OH groups

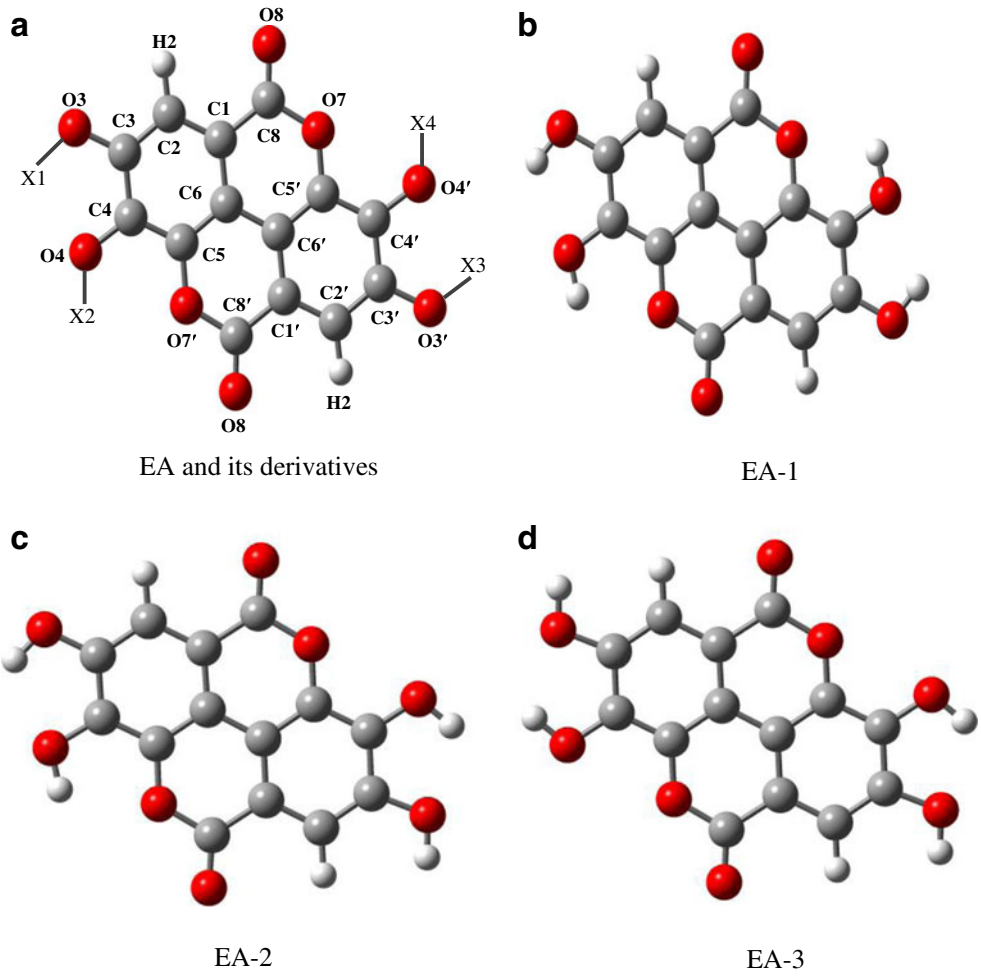

Fig. 1 **a** Atomic numbering and structures of ellagic acid and its three methyl (Me) derivatives. In ellagic acid, X1=X2=X3=X4=H, in 3′-*O*-methyl ellegic acid, X_1=H, X_2=H, X_3=Me, X_4=H, in 3′,4′-di-*O*-methyl ellegic acid, X_1=H, X_2=H, X_3=Me, X_4=Me and in 3,3′-di-*O*-methyl ellegic acid, X_1=Me, X_2=H, X_3=Me, X_4=H. **b**, **c**, **d** Optimized structures of the three conformers of ellagic acid

located on each side of the ring system are oriented in the same direction, so that an intramolecular hydrogen bond is formed between them. These intramolecular hydrogen bonds stabilize the conformers. The relative Gibbs free energies of the three conformers obtained at different levels of theory in the gas phase and aqueous media are presented in Table 1. It is found that, in the gas phase, the conformer EA-1 is most stable at all four levels of theory; in aqueous media, it is most stable at three out of the four levels of theory employed here. As the B3LYP functional is generally rated somewhat better than the B3PW91 functional [62–64], we considered the results obtained at the B3LYP/AUG-cc-pVDZ level to be more reliable than those obtained at the B3PW91/AUG-cc-pVDZ level in aqueous media. Therefore, the conformer EA-1 of ellagic acid was taken to be the most stable. Mono- and dimethyl derivatives of ellagic acid were obtained by appropriate methyl group substitutions in the conformer EA-1 of ellagic acid.

Therefore, the reactions of the free radicals with ellagic acid were studied by considering the conformer EA-1 (Fig. 1b). The optimized gas-phase bond lengths and bond angles involving heavy atoms for the most stable conformer are compared with those observed experimentally using X-ray diffraction [65] in Table S1 (see the "Electronic supplementary material," ESM). The RMS difference between the optimized and XRD bond lengths was found to be 0.025 Å, while

Table 1 Relative Gibbs free energies (ΔG, in kcal/mol) of the three conformers of ellagic acid (EA-1, EA-2, and EA-3) at 298.15 K, obtained at different levels of theory in the gas phase and aqueous media. In each column, the energies are given with respect to that of the conformer EA-1

Conformer	B3LYP/ 6-31G(d,p)	B3PW91/ 6-31G(d,p)	B3LYP/ AUG-cc-pVDZ[a]	B3PW91/ AUG-cc-pVDZ[a]
EA-1	0.00 (0.00)	0.00 (0.00)	0.00 (0.00)	0.00 (0.00)
EA-2	3.31 (0.58)	3.22 (0.46)	3.11 (1.73)	2.81 (−1.02)
EA-3	6.37 (1.23)	6.21 (1.01)	5.97 (2.91)	5.77 (1.40)

The energies given in parentheses correspond to those calculated in aqueous media, while those outside parentheses correspond to those calculated in the gas phase

[a] Single-point energy calculation performed using the corresponding gas-phase optimized geometry

the corresponding difference for bond angles was 0.88°. These differences are within acceptable limits, and can be largely ascribed to the forces present in the crystal environment that are absent from the gas phase.

Barrier energies of hydrogen abstraction reactions

Hydrogen abstraction reactions between ellagic acid or its methyl or dimethyl derivatives [66] and different radicals ($R^{\cdot}$) may be expressed by the following general scheme:

$$A\text{–}H_n + R^{\cdot} \rightarrow A\text{–}H_n\text{–}R^{\cdot} \overset{\Delta G_n^{b}}{\rightarrow} [TS]_n \overset{-\Delta G_n^{r}}{\rightarrow} A^{\cdot}\text{–}R\text{–}H_n,$$

where A–H_n represents ellagic acid or one of its methyl derivatives, and H_n is the hydrogen atom (bonded to the C_n carbon atom) that is to be abstracted by the radical $R^{\cdot}$. In the present study, $R^{\cdot}$ represented a hydroxyl radical, nitrogen dioxide radical, or methoxy radical. The free radical initally forms a reactant complex (RC) with ellagic acid or its methyl or dimethyl derivative (A–H_n–$R^{\cdot}$). Subsequently, after the Gibbs activation energy (ΔG_n^{b}) has become available, a transition state (TS) is formed, which is followed by the formation of the product complex (PC), i.e., $A^{\cdot}$–R–H_n. Thus, at the PC stage (following the abstraction of a hydrogen atom from ellagic acid or one of its methyl or dimethyl derivatives (A–H_n) by an $OH^{\cdot}$, $NO_2^{\cdot}$, or $OCH_3^{\cdot}$ radical), a molecule of water, nitrous acid, or methyl alcohol complexed with a radical of the antioxidant (A·) is formed. Consequent to the formation of the PC, a certain amount of Gibbs free energy ($-\Delta G_n^{r}$) is released. As is well known, hydroxyl groups of phenolic antioxidants play important roles in their antioxidant activities [42]. Because of this, we only considered the abstraction of hydrogen by each of the three radicals from the hydroxyl groups of ellagic acid and its three methyl derivatives.

The hydrogen abstraction reactions with the lowest barrier energies that involve each of the radicals (i.e., $OH^{\cdot}$, $NO_2^{\cdot}$, and $OCH_3^{\cdot}$) along with ellagic acid or 3′-*O*-methyl ellagic acid are shown in Fig. 2, while the corresponding reactions that involve 3,3′-di-*O*-methyl ellegic acid and 3′,4′-di-*O*-methyl ellagic acid are shown in Fig. 3. Thus, only one hydrogen abstraction reaction that involves each of the three radicals and each of the four antioxidant molecules and which corresponds to the lowest barrier energy for that radical–antioxidant combination is shown in each of these two figures. The structures of the RCs, TSs, and PCs along with the barrier and released energies, the important interatomic distances, and the imaginary vibrational frequencies at the TSs involved in these reactions are shown in Figs. 2 and 3.

The ellagic acid molecule is planar and has four hydroxyl groups attached at the C3, C4, C3′, and C4′ positions. Since the structure of the molecule is symmetric, we considered hydrogen abstraction by each of the three radicals from the hydroxyl groups attached at the C3 and C4 positions only. The Gibbs barrier energy and the released energy, denoted ΔG_i^{b} and ΔG_i^{r} (i=3, 4), respectively, for reactions at 298.15 K between ellagic acid (kcal/mol) and each of the three radicals ($OH^{\cdot}$, $NO_2^{\cdot}$, and $OCH_3^{\cdot}$), as obtained at different levels of theory in both the gas phase and aqueous media, are presented in Table 2. The O–H bond lengths of the four antioxidants are increased at the TSs due to the presence of the $OH^{\cdot}$ radical to values of 1.03–1.06 Å; the corresponding lengths in the presence of $OCH_3^{\cdot}$ and $NO_2^{\cdot}$ radicals are 1.09–1.14 Å and 1.12–1.18 Å, respectively (Figs. 2 and 3). The H–O interatomic distances at the TSs in the presence of the $OH^{\cdot}$ radical are 1.40–1.47 Å; the corresponding lengths in the presence of $OCH_3^{\cdot}$ and $NO_2^{\cdot}$ radicals are 1.27–1.32 Å and 1.24–1.30 Å, respectively (Figs. 2 and 3). Thus, the O–H bonds are the longest while the H–O interatomic distances are the shortest at the TSs when the NO_2 group is the reacting radical. The reverse is true for the $OH^{\cdot}$ radical, and the $OCH_3^{\cdot}$ radical lies between the other two radicals in this respect. This correlates with the order of barrier energies, as discussed below.

The Gibbs barrier energies for hydrogen abstraction by an $OH^{\cdot}$ radical from both the C3 and C4 sites in both the gas phase and aqueous media were found to be negative (Table 2). Negative barrier energies imply that hydrogen abstraction from the hydroxyl groups of ellagic acid occurs barrierlessly. The energies released in these reactions in aqueous media, as obtained at different levels of theory, lie in the range −34.5 to −32.1 kcal/mol, showing that the PCs are quite stable. The Gibbs barrier energies associated with the abstraction of hydrogen by $NO_2^{\cdot}$ and $OCH_3^{\cdot}$ radicals in both the gas phase and aqueous media (Table 2) are all positive. The Gibbs barrier energies associated with the abstraction of hydrogen by the $NO_2^{\cdot}$ radical from the hydroxyl groups attached to both the C3 and C4 sites, considering the values calculated in both the gas phase and aqueous media at all four levels of theory employed here, lie in the range 6–14.2 kcal/mol, while those corresponding to hydrogen abstraction by the $OCH_3^{\cdot}$ radical lie in the range 0.4–5 kcal/mol (Table 2). The Gibbs energies released in the reactions involving the $NO_2^{\cdot}$ and $OCH_3^{\cdot}$ radicals are all negative; reactions involving the former radical usually result in more energy being released than those involving the latter do (Table 2).

The Gibbs barrier and released energies of reactions between 3′-*O*-methyl ellagic acid (kcal/mol) and each of the three radicals ($OH^{\cdot}$, $NO_2^{\cdot}$, and $OCH_3^{\cdot}$), as obtained at different levels of theory in both the gas phase and aqueous media, and denoted ΔG_i^{b} and ΔG_i^{r}, respectively (i=3, 4, or 4′), are presented in Table 3. The corresponding results for hydrogen abstraction reactions between 3′,4′-di-*O*-methyl ellagic acid and each of the radicals are presented in Table 4, while those for hydrogen abstraction reactions between 3,3′-di-*O*-methyl ellagic acid and each of the three radicals are presented in Table 5. We can make the following observations based on the

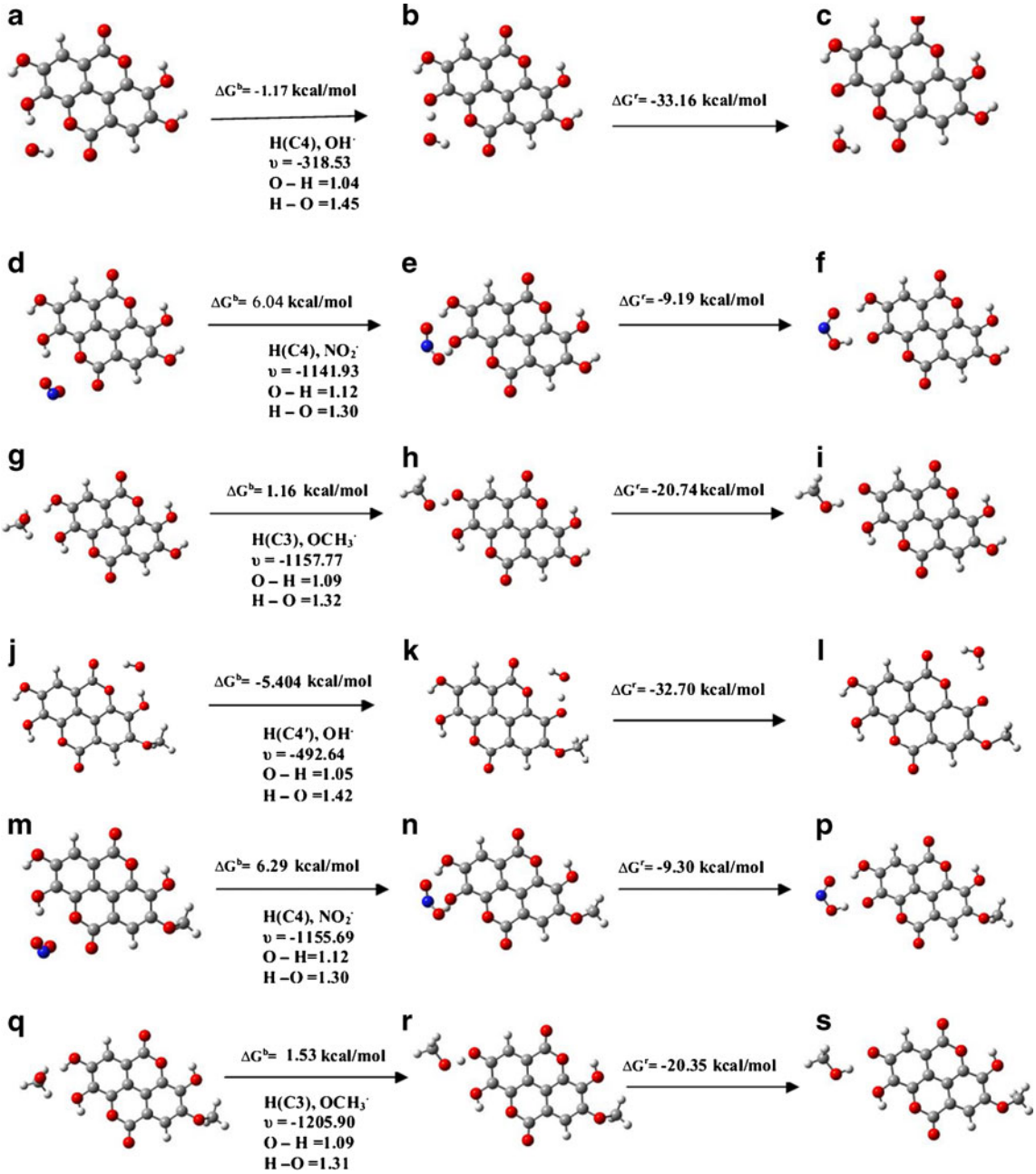

Fig. 2 Gibbs barrier energies the energies released during the scavenging of $OH^{\cdot}$, $NO_2^{\cdot}$ and $OCH_3^{\cdot}$ radicals by ellagic acid or 3′-*O*-methyl ellagic acid. RCs, TSs, and PCs are shown on the left side (a, d, g, j, m, q), in the middle (b, e, h, k, n, r), and on the right side (c, f, i, l, p, s), respectively. The hydrogen atom involved in the reaction, the H attached to C3, C4, or C4′, and the reacting radical are indicated below the *arrow on the left* in each case. The following properties correspond to the transition state in each case: ν is the imaginary frequency (cm^{-1}), *O–H* is the length of the OH bond of ellagic acid or 3′-*O*-methyl ellagic acid, *H* is the hydrogen atom that is abstracted (Å), and *H–O* is the distance between the hydrogen atom abstracted and the oxygen atom of the radical under consideration

results presented in Tables 3, 4, and 5. The Gibbs barrier energy for the reaction between the mono- or dimethyl ellagic acid molecule and the $OH^{\cdot}$ or $NO_2^{\cdot}$ radical is usually similar to that between ellagic acid and the corresponding radical. The Gibbs barrier energy for the abstraction of hydrogen from the C3 site of the mono- or dimethyl ellagic acid molecule and the $OCH_3^{\cdot}$ radical is also similar to that for the reaction between ellagic acid and the same radical. However, the Gibbs barrier energies for the corresponding reactions from the C4 sites of the antioxidant molecules and the $OCH_3^{\cdot}$ radical are appreciably larger than those for the reactions between ellagic acid and the corresponding radicals. The reason for this difference is that, at the RC corresponding to the abstraction of hydrogen from the C4 site, one of the hydrogen atoms of the OCH_3

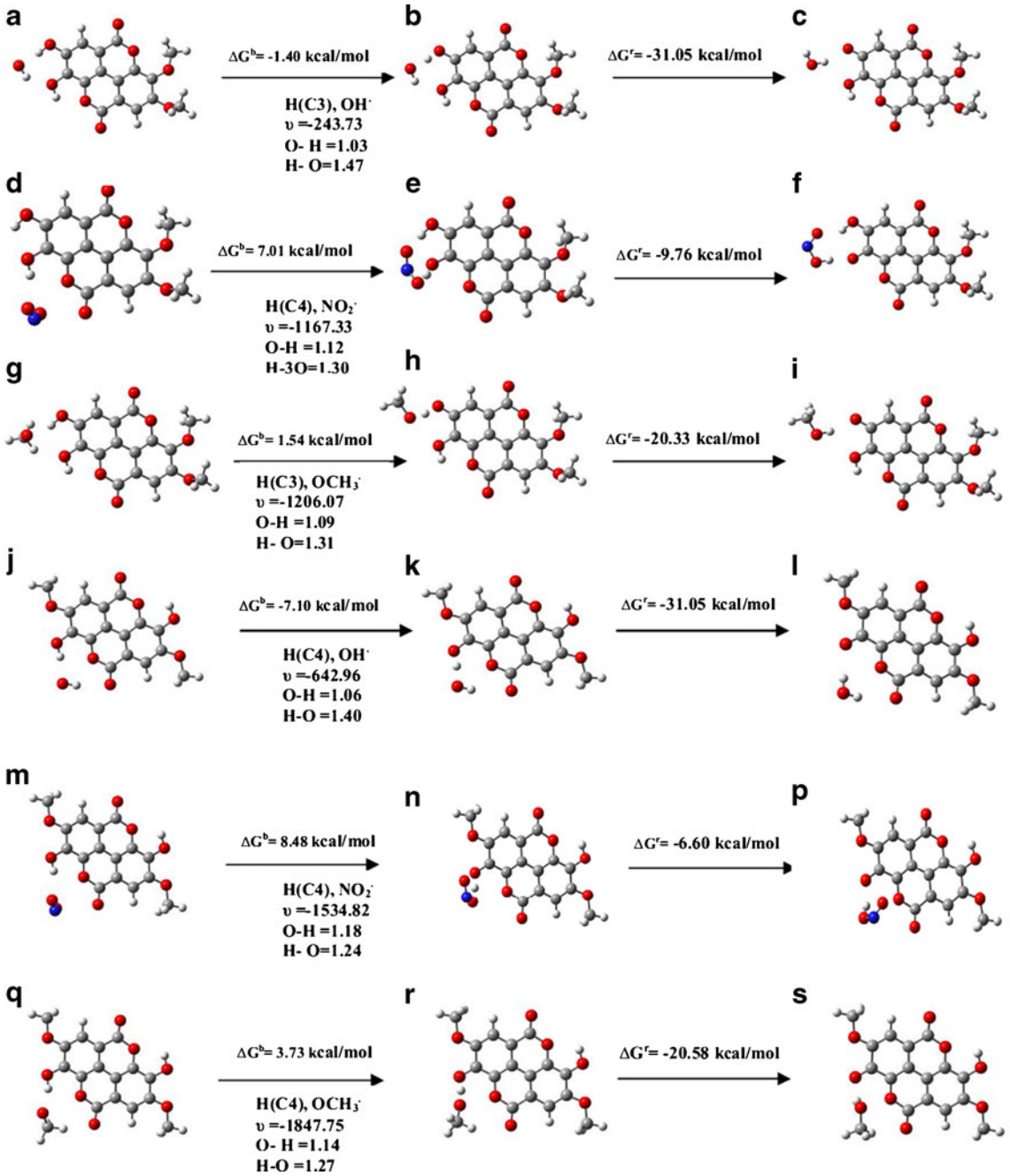

Fig. 3 Gibbs barrier energies the energies released during the scavenging of $OH^{\cdot}$, $NO_2^{\cdot}$, and $OCH_3^{\cdot}$ radicals by 3′,4′-di-*O*-methyl ellagic acid or 3,3′-di-*O*-methyl ellagic acid. RCs, TSs, and PCs are shown on the left side (*a*, *d*, *g*, *j*, *m*, *q*), in the middle (*b*, *e*, *h*, *k*, *n*, *r*), and on the right side (*c*, *f*, *i*, *l*, *p*, *s*), respectively. The hydrogen atom involved in the reaction, the H attached to C3 or C4, and the reacting radical are indicated below the *arrow on the left* in each case. The following properties correspond to the transition state in each case: ν is the imaginary frequency (cm^{-1}), *O–H* is the length of the OH bond of 3′,4′-di-*O*-methyl ellagic acid or 3,3′-di-*O*-methyl ellagic acid, *H* is the hydrogen atom that is abstracted (Å), and H–O is the distance between the hydrogen atom abstracted and the oxygen atom of the radical under consideration

group, bearing a Mulliken charge of 0.204, is involved in hydrogen bonding with the O8′ (Mulliken charge −0.491) and O7′ (Mulliken charge −0.565) sites of the antioxidant molecules (Figs. 1a and 2q). Because of this, the RC corresponding to hydrogen abstraction by $OCH_3^{\cdot}$ from the C4 site is appreciably more stabilized than that corresponding to hydrogen abstraction from the C3 site by the same radical. As the RC is appreciably more stabilized in this case, the barrier energy is significantly increased.

Barrier energies for the abstraction of hydrogen by the hydroxyl radical from ellagic acid and its mono- as well as dimethyl derivatives were also calculated in terms of enthalpy. These barrier energies (Table S2 of the ESM) were also found to be negative, just as those calculated in terms of the Gibbs

Table 2 Gibbs barrier energies (ΔG_i^{b}, i=3, 4, in kcal/mol) and released energies (ΔG_i^{r}, i=3, 4, in kcal/mol) at 298.15 K for the abstraction of hydrogen by $OH^{\cdot}$, $NO_2^{\cdot}$, or $OCH_3^{\cdot}$ radicals from different sites on ellagic acid, as obtained at different levels of theory in the gas phase and aqueous media (results calculated in aqueous media are shown in parentheses)

Free radical	Gibbs energy[a]	B3LYP/6-31G(d,p)	B3LYP/AUG-cc-pVDZ[c]	B3PW91/6-31G(d,p)[c]	B3PW91/AUG-cc-pVDZ[c]
$OH^{\cdot}$	ΔG_3^{b}	−0.6 (−1.0)	−0.8 (−1.0)	−0.5 (−0.6)	−1.6 (−1.5)
	ΔG_3^{r}	−28.1 (−32.8)	−29.05 (−32.1)	−28.01 (−32.8)	−30.42 (−34.3)
	ΔG_4^{b}	−0.7 (−1.2)	−0.4 (−2.6)	−0.6 (−0.8)	−1.5 (−1.1)
	ΔG_4^{r}	−28.3 (−33.2)	−30.6 (−33.5)	−28.2 (−33.1)	−30.5 (−34.5)
$NO_2^{\cdot}$	ΔG_3^{b}	11.2 (7.5)	13.5 (8.6)	12.1 (8.9)	13.5 (12.5)
	ΔG_3^{r}	−7.4 (−7.0)	−9.8 (−20.7)	−6.0 (−5.9)	−6.2 (−4.7)
	ΔG_4^{b}	8.5 (6.0)	13.3 (9.8)	9.2 (7.2)	11.6 (14.2)
	ΔG_4^{r}	−9.5 (−9.2)	−12.8 (−12.0)	−8.4 (−8.2)	−30.2 (−10.8)
$OCH_3^{\cdot}$	ΔG_3^{b}	1.0 (1.2)	3.2 (3.3)	0.9 (1.1)	0.4 (2.6)
	ΔG_3^{r}	−17.1(−20.7)	−27.6 (−19.9)	−16.5 (−20.1)	−17.5 (−21.0)
	ΔG_4^{b}	2.5 (2.1)	4.2 (5.0)	2.3 (2.0)	2.0 (2.7)
	ΔG_4^{r}	−16.9 (−19.3)	−22.0 (−19.8)	−16.2 (−18.6)	−16.7 (−18.7)

[a] The superscripts "b" and "r" refer to the Gibbs barrier energy and the released energy, respectively. The subscripts "3" and "4" refer to the site that the hydrogen is abstracted from

[c] Obtained from single-point energy calculations using the B3LYP/6-31G(d,p)-level optimized geometries

free energy were, and so they support the conclusion that the reactions under consideration are barrierless.

The reactivities of the radicals, as indicated by the barrier energies for all four antioxidant molecules, decrease in the order $OH^{\cdot} > OCH_3^{\cdot} > NO_2^{\cdot}$ [49]. A graphical presentation of the Gibbs barrier energies involved in the abstraction of hydrogen by hydroxyl, nitrogen dioxide, and methoxy radicals from the C3 and C4 sites of ellagic acid and its mono- and

Table 3 Gibbs free barrier energies (ΔG_i^{b}, i=3, 4, or 4′, in kcal/mol) and released energies (ΔG_i^{r}, i =3, 4, or 4′, in kcal/mol) at 298.15 K for the abstraction of hydrogen by $OH^{\cdot}$, $NO_2^{\cdot}$, and $OCH_3^{\cdot}$ radicals from different sites on 3′-*O*-methyl ellagic acid, as obtained at different levels of theory in the gas phase and aqueous media (results calculated in aqueous media are given in parentheses)

Free radical	Gibbs energy[a]	B3LYP/6-31G(d,p)	B3LYP/AUG-cc-pVDZ[c]	B3PW91/6-31G(d,p)[c]	B3PW91/AUG-cc-pVDZ[c]
$OH^{\cdot}$	ΔG_3^{b}	−1.3 (−1.6)	−4.6 (−7.0)	−1.2 (−1.2)	−5.4 (−6.8)
	ΔG_3^{r}	−26.9 (−31.2)	−15.9 (−31.1)	−26.8 (−31.2)	−25.9 (−31.2)
	ΔG_4^{b}	−0.9 (−1.2)	−6.3 (−1.9)	−0.8 (−0.9)	−6.4 (−1.3)
	ΔG_4^{r}	−28.4 (−33.2)	−30.7 (−33.9)	−28.3 (−33.1)	−30.7 (−34.1)
	$\Delta G_{4'}^{b}$	0.0 (−5.4)	−1.4 (−6.3)	0.2 (−5.2)	−1.0 (−5.8)
	$\Delta G_{4'}^{r}$	−27.9 (−32.7)	−30.2 (−32.2)	−27.7 (−32.6)	−30.0 (−32.3)
$NO_2^{\cdot}$	ΔG_3^{b}	11.6 (8.4)	13.2 (15.5)	12.5 (9.8)	13.7 (16.4)
	ΔG_3^{r}	−7.5 (−7.2)	−7.8 (−6.9)	−6.1 (−6.1)	−6.3 (−5.8)
	ΔG_4^{b}	8.2 (6.3)	10.7 (11.2)	8.9 (7.4)	11.1 (11.8)
	ΔG_4^{r}	−9.3 (−9.3)	−10.6 (−10.7)	−8.1 (−8.3)	−9.2 (−9.3)
	$\Delta G_{4'}^{b}$	10.7 (7.5)	12.4 (12.7)	11.4 (8.7)	13.1 (13.4)
	$\Delta G_{4'}^{r}$	−8.5 (−10.6)	−9.1 (−9.3)	−7.3 (−7.5)	−7.9 (−8.2)
$OCH_3^{\cdot}$	ΔG_3^{b}	1.2 (1.5)	0.7 (3.1)	1.0 (1.4)	0.6 (3.0)
	ΔG_3^{r}	−17.0 (−20.4)	−18.3 (−19.0)	−16.4 (−19.7)	−17.7 (−18.5)
	ΔG_4^{b}	2.6 (2.2)	9.2 (2.7)	2.3 (2.0)	8.6 (2.4)
	ΔG_4^{r}	−17.0 (−19.3)	−24.3 (−18.2)	−16.2 (−18.4)	−23.3 (−17.6)
	$\Delta G_{4'}^{b}$	4.6 (4.3)	5.3 (6.8)	4.4 (4.3)	9.9 (6.3)
	$\Delta G_{4'}^{r}$	−19.2 (−22.1)	−21.0 (−22.0)	−18.5 (−21.5)	−25.1 (−21.0)

[a] The superscripts "b" and "r" refer to the Gibbs barrier energy and the released energy, respectively. The subscripts "3," "4," and "4′ " refer to the site that the hydrogen is abstracted from

[c] Obtained from single-point energy calculations using the B3LYP/6-31G(d,p)-level optimized geometries

Table 4 Gibbs free barrier energies (ΔG_i^{b}, i =3, 4, in kcal/mol) and released energies (ΔG_i^{r}, i =3, 4, in kcal/mol) at 298.15 K for the abstraction of hydrogen by $OH^{\cdot}$, $NO_2^{\cdot}$, or $OCH_3^{\cdot}$ radicals from different sites on 3′,4′-di-*O*-methyl ellagic acid, as obtained at different levels of theory in the gas phase and aqueous media (results calculated in aqueous media are given in parentheses)

Free radical	Gibbs energy[a]	B3LYP/6- 31G(d,p)	B3LYP/AUG-cc-pVDZ[c]	B3PW91/6-31G(d,p)[c]	B3PW91/AUG- cc-pVDZ[c]
$OH^{\cdot}$	ΔG_3^{b}	−1.1 (−1.4)	−3.3 (−3.2)	−0.9 (−1.0)	−8.0 (−2.5)
	ΔG_3^{r}	−27.1 (−31.1)	−28.0 (−33.5)	−27.2 (−31.2)	−29.9 (−33.7)
	ΔG_4^{b}	−0.7 (−1.0)	−6.2 (0.0)	−0.6 (−0.7)	−6.2 (0.4)
	ΔG_4^{r}	−28.5 (−48.1)	−30.7 (−35.8)	−28.4 (−33.1)	−30.8 (−35.6)
$NO_2^{\cdot}$	ΔG_3^{b}	11.3 (8.3)	12.9 (10.2)	12.3 (9.7)	13.6 (11.4)
	ΔG_3^{r}	−7.3 (−7.1)	−7.7 (−3.4)	−5.9 (−6.0)	−6.2 (−2.7)
	ΔG_4^{b}	8.7 (7.0)	11.2 (14.9)	9.4 (8.1)	11.5 (15.3)
	ΔG_4^{r}	−9.7 (−9.8)	−11.0 (−10.4)	−8.5 (−8.7)	−9.6 (−9.0)
$OCH_3^{\cdot}$	ΔG_3^{b}	1.2 (1.5)	0.7 (1.7)	1.1 (1.1)	0.5 (1.4)
	ΔG_3^{r}	−16.9 (−20.3)	−18.2 (−18.6)	−16.4 (−16.4)	−17.4 (−17.9)
	ΔG_4^{b}	2.6 (2.3)	2.3 (4.4)	2.3 (2.3)	8.5 (4.1)
	ΔG_4^{r}	−17.2 (−19.4)	−17.6 (−19.6)	−16.5 (−16.5)	−23.6 (−18.9)

[a] The superscripts "b" and "r" refer to the Gibbs barrier energy and the released energy, respectively. The subscripts "3" and "4" refer to the site that the hydrogen is abstracted from

[c] Obtained from single-point energy calculations using the B3LYP/6-31G(d,p)-level optimized geometries

dimethyl derivatives in aqueous media is given in Fig. 4. This enables a convenient comparison of the Gibbs barrier energies associated with the abstraction of hydrogen from ellagic acid and its methyl derivatives by the three radicals. It is obvious from this figure that hydrogen abstraction by an $OH^{\cdot}$ radical from the hydroxyl groups of ellagic acid and its methyl derivatives in aqueous media would be barrierless, while the Gibbs barrier energies would be small or moderate (~1–4 kcal/mol) or fairly large (~6–8 kcal/mol) in the same medium when the radical involved is $NO_2^{\cdot}$ or $OCH_3^{\cdot}$, respectively.

Rate constants for hydrogen abstraction reactions

According to transition state theory [59], the rate constant for a chemical reaction is given by

$$K = (K_B T/h)\exp\left(-\Delta G^{b}/RT,\right)$$

where K is the thermal rate constant, K_B is the Boltzmann constant, T is the absolute temperature (298.15 K), h is Planck's constant, R is the gas constant, and ΔG^{b} is the Gibbs barrier energy involved in the reaction under consideration. Ideally, the above expression should also be multiplied by a tunneling factor, but this factor is very close to 1, so it was ignored here. The calculated rate constants for the abstraction of hydrogen at 298.15 K by $OH^{\cdot}$, $NO_2^{\cdot}$, and $OCH_3^{\cdot}$ radicals from different sites on ellagic acid and its monomethyl and dimethyl derivatives, as calculated at the B3LYP/6-31G(d,p) and B3PW91/6-31G(d,p) levels of density functional theory in the gas phase (R_i^{G}) and aqueous media (R_i^{A}, where the subscript i corresponds to the number label of the oxygen

Table 5 Gibbs free barrier energies (ΔG_4^{b}, in kcal/mol) and released energies (ΔG_4^{r}, in kcal/mol) at 298.15 K for the abstraction of hydrogen by $OH^{\cdot}$, $NO_2^{\cdot}$, or $OCH_3^{\cdot}$ radicals from different sites on 3,3′-di-*O*-methyl ellagic acid, as obtained at different levels of theory in the gas phase and aqueous media (results calculated in aqueous media are given in parentheses)

Free radical	Gibbs energy[a]	B3LYP/6- 31G(d,p)	B3LYP/AUG-cc-pVDZ[c]	B3PW91/6-31 G(d,p)[c]	B3PW91/AUG-cc-pVDZ[c]
$OH^{\cdot}$	ΔG_4^{b}	−0.7 (−7.1)	−5.5 (−8.3)	−5.5 (−8.3)	−1.8 (−7.9)
	ΔG_4^{r}	−26.1 (−31.1)	−28.3 (−29.7)	−28.3 (−29.7)	−28.1 (−29.8)
$NO_2^{\cdot}$	ΔG_4^{b}	10.9 (8.5)	13.5 (17.0)	12.3 (10.5)	14.6 (18.1)
	ΔG_4^{r}	−7.3 (−6.6)	−7.4 (−7.6)	−5.9 (−5.6)	−6.0 (−6.2)
$OCH_3^{\cdot}$	ΔG_4^{b}	4.9 (3.7)	10.9 (5.6)	4.8 (3.8)	10.7 (5.1)
	ΔG_4^{r}	−17.7 (−20.6)	−24.7 (−21.5)	−16.9 (−19.9)	−23.9 (−20.7)

[a] The superscripts "b" and "r" refer to the Gibbs barrier energy and the released energy, respectively. The subscript "4′" refers to the site that the hydrogen is abstracted from

[c] Obtained from single-point energy calculations using the B3LYP/6-31G(d,p)-level optimized geometries

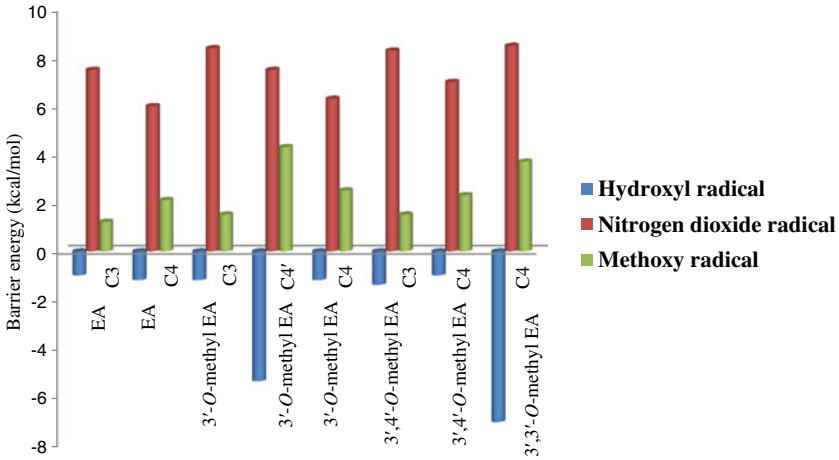

Fig. 4 Graphical representation of the Gibbs barrier energies (kcal/mol) associated with the abstraction of hydrogen from ellagic acid and its three methyl derivatives by hydroxyl, nitrogen dioxide, and methoxy radicals in aqueous media. Here C3, C4, and C4′ are the sites from which the hydrogen is abstracted

atom to which the hydrogen atom to be abstracted is attached), are given in Table S3 of the ESM, while the corresponding results obtained at the B3LYP/AUG-cc-pVDZ and B3PW91/AUG-cc-pVDZ levels of theory are given in Table 6. We can make the following observations based on the results presented in Tables S3 and 6. (i) When $NO_2^{\cdot}$ is the hydrogen-abstracting radical, the rate constants in the gas phase or aqueous media obtained using the AUG-cc-pVDZ basis set in some cases are appreciably smaller than those obtained using the 6-31G(d,p) basis set. However, when $OH^{\cdot}$ and $OCH_3^{\cdot}$ are the hydrogen-abstracting radicals, the rate constants obtained using the AUG-cc-pVDZ and 6-31G(d,p) basis sets are similar. (ii) In many cases, the rate constants substantially increase upon going from the gas phase to aqueous media, although the reverse is also true in a few cases.

The rate constants for the scavenging of OH radicals by ellagic acid and its monomethyl and dimethyl derivatives are

Table 6 Rate constants in the gas phase (R_i^G, i =3, 4, or 4′, in $M^{-1}S^{-1}$) and aqueous media (R_i^A, i =3, 4, or 4′, in $M^{-1}S^{-1}$) at 298.15 K for the abstraction of hydrogen by $OH^{\cdot}$, $NO_2^{\cdot}$, or $OCH_3^{\cdot}$ radicals from different sites on ellagic acid and its monomethyl and dimethyl derivatives, as obtained at the B3LYP/AUG-cc-pVDZ and B3PW91/AUG-cc-pVDZ levels of theory (results calculated at the B3PW91/AUG-cc-pVDZ level are given in parentheses)

Free radical	Rate constant[a]	Ellagic acid	3′-*O*-methyl ellagic acid	3′,4′-Di-*O*-methyl ellagic acid	3,3′-Di-*O*-methyl ellagic acid
$OH^{\cdot}$	R_3^G	2.4×10^{13} (9.2×10^{13})	1.5×10^{16} (5.7×10^{16})	1.6×10^{15} (4.3×10^{18})	
	R_3^A	3.4×10^{13} (7.8×10^{13})	8.4×10^{17} (6.0×10^{17})	1.4×10^{15} (4.2×10^{14})	
	R_4^G	1.2×10^{13} (7.8×10^{13})	2.6×10^{17} (3.0×10^{17})	2.2×10^{17} (2.2×10^{17})	6.7×10^{16} (1.3×10^{14})
	R_4^A	5.0×10^{14} (3.9×10^{13})	1.5×10^{14} (5.6×10^{13})	6.2×10^{12} (3.2×10^{12})	7.6×10^{18} (3.9×10^{18})
	$R_{4'}^G$		6.6×10^{13} (3.4×10^{13})		
	$R_{4'}^A$		2.6×10^{17} (1.1×10^{17})		
$NO_2^{\cdot}$	R_3^G	7.8×10^{2} (7.8×10^{2})	1.2×10^{3} (5.5×10^{2})	2.1×10^{3} (6.6×10^{2})	
	R_3^A	3.1×10^{7} (4.2×10^{3})	4.4×10^{2} (5.8)	2.0×10^{5} (2.7×10^{4})	
	R_4^G	1.1×10^{3} (1.9×10^{4})	8.8×10^{4} (4.5×10^{4})	3.8×10^{4} (2.3×10^{4})	7.8×10^{2} (1.2×10^{2})
	R_4^A	4.0×10^{5} (2.4×10^{2})	3.8×10^{4} (1.4×10^{4})	7.3×10^{1} (3.7×10^{1})	2.1 (3.2)
	$R_{4'}^G$		5.0×10^{3} (1.5×10^{3})		
	$R_{4'}^A$		3.0×10^{3} (9.2×10^{2})		
$OCH_3^{\cdot}$	R_3^G	2.8×10^{10} (3.2×10^{12})	1.9×10^{12} (2.2×10^{12})	1.9×10^{12} (2.7×10^{12})	
	R_3^A	2.4×10^{10} (7.7×10^{10})	3.3×10^{10} (3.9×10^{10})	3.5×10^{11} (5.8×10^{11})	
	R_4^G	5.2×10^{9} (7.7×10^{10})	1.1×10^{6} (3.0×10^{6})	1.3×10^{11} (3.6×10^{6})	6.2×10^{4} (1.2×10^{5})
	R_4^A	1.3×10^{9} (6.5×10^{10})	6.5×10^{10} (1.1×10^{11})	3.7×10^{9} (6.1×10^{9})	4.8×10^{8} (1.1×10^{9})
	$R_{4'}^G$		6.4×10^{7} (1.5×10^{8})		
	$R_{4'}^A$		8.0×10^{8} (3.3×10^{5})		

[a] The superscripts "G" and "A" refer to the gas phase and aqueous media, respectively. The subscripts "3," "4," or "4′" refer to the site that the hydrogen is abstracted from

mostly found to be on the order of 10^{13} $M^{-1}S^{-1}$ or more in the gas phase, while those calculated in aqueous media lie mostly in the range 10^{13}–10^{16} $M^{-1}S^{-1}$. When $OCH_3^{\cdot}$ is the hydrogen-abstracting radical, the rate constants in the gas phase lie in the broad range of 10^9 to 10^{12} M^{-1} S^{-1} while those in aqueous media lie in the broad range of 10^8 to 10^{12} M^{-1} S^{-1}. When $NO_2^{\cdot}$ is the hydrogen-abstracting radical, the rate constants in the gas phase are found to be quite small, lying in the range 10^4 to 10^6 M^{-1} S^{-1}, while those in aqueous media mostly lie in the range 10^4 to 10^8 M^{-1} S^{-1}. However, in some cases when $NO_2^{\cdot}$ is the hydrogen-abstracting radical, the rate constants in aqueous media are quite small. Rate constants for hydrogen abstraction by $OH^{\cdot}$ and $NO_2^{\cdot}$ radicals have been determined experimentally at pH 7 and 8.5 [49]. Our calculated rate constants, particularly those obtained at the B3LYP/6-31G(d,p) and B3PW91/6-31G(d,p) levels in the gas phase, are quite similar to those obtained experimentally [49]. The calculated rate constants show that ellagic acid and its monomethyl and dimethyl derivatives are good radical scavengers, and their scavenging rates decrease in the order $OH^{\cdot}$ >> $OCH_3^{\cdot}$ > $NO_2^{\cdot}$. Nitrogen dioxide ($NO_2^{\cdot}$) is one of the most reactive species in the RNOS family [17, 49]. However, as shown by the results discussed above, it would be less efficiently scavenged by ellagic acid than $OH^{\cdot}$ and $OCH_3^{\cdot}$. Therefore, it appears that RNOS would, in general, be less efficiently scavenged than ROS.

Effect of specific water molecules on the barrier energy

We examined the possible roles of specific water molecules located near the reaction sites in two representative cases. One of these two cases was that of ellagic acid, where the Gibbs barrier energy was more negative than the other one for the same molecule, while the other case was that of 3′-*O*-methyl ellagic acid, where the Gibbs barrier energy was the most negative of all the cases considered in the present study. We studied the mechanisms of these two reactions by placing two specific water molecules near the reaction sites and fully optimizing the corresponding reactant complexes, transition states, and product complexes. It was found that the two specific water molecules stabilized the reactant complexes but did not interfere with the reaction mechanisms, as shown in Fig. S1a–f of the ESM. Consequently, the barrier energies in the cases of ellagic acid and 3′-*O*-methyl ellagic acid increased somewhat, becoming small positive (i.e., 0.74 and 1.02 kcal/mol) from small negative (i.e., −0.6 and −1.3 kcal/mol, respectively). Thus we find that including specific water molecules does not alter the reaction mechanism, although it does increase the barrier energy by a small amount. It is expected that similar situations will also occur in the other cases.

Single electron transfer reactions

We considered single electron transfer from ellagic acid or any of its monomethyl and dimethyl derivatives (A) to any of the three radicals ($R^{\cdot}$) considered here [66]. Electron transfer reactions may be expressed by the following general scheme:

$$A + R^{\cdot} \xrightarrow{AIP} A^{\cdot+} + R^{-}.$$

In this reaction, ellagic acid or any of its monomethyl or dimethyl derivatives (A) acts as an electron donor while the radical ($R^{\cdot}$) acts as an electron acceptor. The possibility of single electron transfer reactions can be studied using the adiabatic ionization potential (AIP). The value of this parameter was calculated for ellagic acid and all of its methyl derivatives mentioned above in combination with each of the three radicals considered here in both the gas phase and aqueous media at different levels of theory, and the results are presented in Table S4 of the ESM. We note the following from this table. (i) The AIP values are appreciably sensitive to the density functional and basis set used. (ii) In most cases, the AIP values in the gas phase are quite large. This suggests that the electron transfer mechanism is barely operative in the gas phase, except, say, in the presence of ionizing radiation. (iii) The AIP values in aqueous media are much less than those in the gas phase in all cases. Therefore, the electron transfer process would be much more likely to occur in aqueous media than in the gas phase. Further, the AIP values obtained at the B3LYP/AUG-cc-pVDZ and B3PW91/AUG-cc-pVDZ levels in aqueous media for the OH radical are negative, while those obtained using the same functionals and the 6-31G(d,p) basis set are positive. If we consider the values obtained using the AUG-cc-pVDZ basis set, the present results (Table S4 of the ESM) show that the electron transfer mechanism involving any of the antioxidant molecules and the OH radical would occur very efficiently in aqueous media, but the same processes involving the other two radicals would be much less efficient, even in aqueous media.

Spin density and molecular electrostatic potential distributions

Spin density distributions in the various RCs, TSs, and PCs corresponding to hydrogen abstraction by $OH^{\cdot}$, $NO_2^{\cdot}$, and $OCH_3^{\cdot}$ radicals at the C3 and C4 sites of ellagic acid for the iso-spin density value of 0.001 electrons/bohr^3 are presented in Fig. S2 of the ESM. In this figure, the spin density distributions in RCs, TSs, and PCs are shown on the left side, in the middle, and on the right side in each case, respectively. Molecular electrostatic potential (MEP) distributions in the same RCs, TSs, and PCs (Fig. S3 of the ESM) corresponding to

hydrogen abstraction by the same three radicals at the same sites of ellagic acid for the iso-MEP values of ±15.7 kcal/mol are presented in Fig. S3 of the ESM. In this figure, the pink and yellow colors correspond to negative and positive MEP values, respectively. It should be noted that spin density is localized at the attacking radicals in the various RCs, while it is usually delocalized over fairly broad regions including the radicals and ellagic acid at the TSs (Fig. S2 of the ESM). Also, at the PCs, spin density is delocalized over fairly extended regions of the ellagic acid radical created by the loss of a hydrogen atom from ellagic acid. Further, at the PCs, spin density is most pronounced near the site on ellagic acid from which the hydrogen atom is abstracted.

It is well established that negative MEP is a sensitive indicator of electron density. At the RCs of reactions involving the attack of an $OH^{\cdot}$ radical on ellagic acid (Fig. S3a, d of the ESM), the negative-MEP regions for the chosen MEP value are pronounced near the carbonyl group oxygen atoms, the oxygen atoms of the OH groups attached to the C3 and C3′ sites of ellagic acid, and near the oxygen atom of the attacking $OH^{\cdot}$ radical. Broadly speaking, the same is true for the corresponding transition states (Fig. S3b, e of the ESM), while, at the PCs, fairly broad negative-MEP regions are localized near the sites from which hydrogen atoms are abstracted. At the RCs of reactions involving the $NO_2^{\cdot}$ radical (Fig. S3g, j of the ESM), no negative-MEP region is located near this radical, but such regions are located on the corresponding TSs (Fig. S3h, k of the ESM). At the PCs, negative-MEP regions are located near HNO_2, which is formed from the $NO_2^{\cdot}$ radical after this radical abstracts a hydrogen atom. In this case, an extended negative-MEP region is also located near the site from which hydrogen is abstracted. At the RCs and TSs of reactions involving the attack of the $OCH_3^{\cdot}$ radical on ellagic acid (Fig. S3m, q of the ESM), negative-MEP regions are located mainly near the oxygen atom of this radical, the carbonyl group oxygen atoms, and the oxygen atoms of the hydroxyl groups attached to C3 and C3′. At the PCs formed due to the reaction of the $OCH_3^{\cdot}$ radical with ellagic acid (Fig. S3p, s of the ESM), broad negative-MEP regions occur near the regions from which hydrogen was abstracted in each case. Thus, we find that both spin density and MEP are distributed over broad regions near the site at which hydrogen abstraction occur. This shows that the sites from which hydrogen atoms are abstracted are quite reactive and would readily capture hydrogen atoms, if available.

Conclusions

We can draw the following conclusion from theGibbs barrier energies and rate constants calculated in the present work. The Gibbs barrier energies involved in the abstraction of hydrogen by an $OH^{\cdot}$ radical from the hydroxyl groups of ellagic acid and its monomethyl and dimethyl derivatives in both the gas phase and aqueous media were all found to be negative, which implies that the reactions are barrierless, and the corresponding rate constants, including those calculated in gas phase and aqueous media, are in the range 10^{13}–10^{16} M^{-1} S^{-1}. Therefore, these reactions would occur very efficiently. Specific water molecules located near the reaction sites increase barrier heights by ~1–2 kcal/mol by stabilizing reactant complexes, but they do not interfere with the reaction mechanisms. The Gibbs barrier energies are moderately to notably large and positive when the radical involved in the hydrogen abstraction reactions is $OCH_3\cdot$. In this case, the rate constants, including those calculated in both the gas phase and aqueous media, lie in the range 10^{8}–10^{12} M^{-1} S^{-1}. When $NO_2^{\cdot}$ is the radical involved in hydrogen abstraction, barrier energies are appreciably increased, meaning that the rate constants mostly lie in the range 10^{4}–10^{8} M^{-1} S^{-1}, although, in some cases, the rate constants are much smaller. Hence, the scavenging efficiencies of ellagic acid and its monomethyl and dimethyl derivatives towards the three radicals decrease in the order $OH^{\cdot}$ >> $OCH_3^{\cdot}$ > $NO_2^{\cdot}$. The available experimental results on the scavenging rate constants of ellagic acid towards $OH^{\cdot}$ and $NO_2^{\cdot}$ radicals broadly agree with our theoretical results.

Acknowledgments The authors are thankful to the University Grants Commission (New Delhi) for financial support.

References

1. Wiseman H, Halliwell B (1996) J Biochem 313:17–29
2. Marnett LJ (2000) Carcinogenesis 21:361–370
3. Hussain SP, Hofseth LJ, Harris CC (2003) Nat Rev Cancer 3:276–285
4. Loft S, Poulsen HE (2006) J Mol Med 74:297–312
5. Doll R, Peto R (1981) J Natl Cancer Inst 66:1191–1308
6. Chakraborty P, Kumar S, Dutta D, Gupta V (2009) J Pharm Tech 2: 238–244
7. Ames BN, Shigenaga MK, Hagen TM (1993) Proc Natl Acad Sci U S A 90:7915–7922
8. Mecocci P, Fano G, Fulle S, Macgarvey U, Shinobu L, Polidori MC, Cherubini A, Vecchiet J, Senin U, Beal MF (1999) Free Rad Biol Med 26:303–308
9. Mecocci P, MacGarvey U, Kaufman AE, Koontz D, Shoffner JM, Wallace DC, Beal MF (1993) Annal Neurol 34:609–616
10. Squadrito GL, Pryor WA (1998) Free Rad Biol Med 25:392–403
11. Halliwell B, Gutterridge JMC (1984) J Biochem 219:1–14
12. Yarkony DR, Schaefer HF, Rothenberg S (1974) J Am Chem Soc 96: 656–659
13. Halliwell B (1999) Mut Res 443:37–52
14. Pryor WA, Stone K (1993) Ann NY Acad Sci 686:12–28
15. Augusto O, Bonini MG, Amanso AM, Linares E, Santos CCX, Menezes LD (2002) Free Rad Biol Med 32:841–859
16. Shukla PK, Mishra PC (2008) J Phys Chem B 112:4779–4789
17. Niles JC, Wishnok JS, Tannenbaum SR (2006) Nitric Oxide 14:109–121
18. Sodum RS, Fiala ES (2001) Chem Res Toxicol 14:438–450
19. Pavlovic R, Santaniello E (2007) J Pharm Pharmacol 59:1687–1695

20. Jena NR, Mishra PC, Suhai S (2009) J Phys Chem B 113:5633–5644
21. Agnihotri N, Mishra PC (2009) J Phys Chem B 113:3129–3138
22. Agnihotri N, Mishra PC (2010) J Phys Chem B 114:7391–7404
23. Shukla MK, Mishra PC (1995) Spectrochim Acta A 51:831–838
24. Agnihotri N, Mishra PC (2009) J Phys Chem B 113:12096–12104
25. Tiwari S, Mishra PC (2011) J Mol Model 17:59–72
26. Shukla MK, Mishra PC (1996) J Mol Struct (Theochem) 377:247–259
27. Shukla PK, Mishra PC (2007) J Phys Chem B 111:4603–4615
28. Yadav A, Mishra PC (2012) Chem Phys 405:76–88
29. Yadav A, Mishra PC (2013) J Mol Model 19:767–777
30. Galano A, Alvarez-Idaboy JR (2011) R Soc Chem 1:1763–1771
31. Agnihotri N, Mishra PC (2011) J Phys Chem A 115:14221–14232
32. Mates JM, Perez-Gomez C, de Castro IN (1999) Clin Biochem 32: 595–603
33. Mullen W, McGinn J, Lean ME, MacLean MR, Gardner P, Duthie GG, Yokota T, Crozier A (2002) J Agric Food Chem 50:5191–5196
34. Radtke J, Linseisen J, Wolfram G (1998) Ernaehrungswiss 37:190–197
35. Mohajeri A, Asemani SS (2009) J Mol Struct 930:15–20
36. Vattem DA, Shetty K (2005) J Food Biochem 29:234–266
37. Da Silva SL, Calgarotto AK, Chaar JS, Marangoni S (2008) Toxicon 52:655–666
38. Zafrilla P, Ferreres F, Francisco AT (2001) J Agric Food Chem 49: 3651–3655
39. Ancos B, Gonzalez EM, Cano P (2000) J Agric Food Chem 48: 4565–4570
40. Hakkinen SH, Karenlampi SO, Mykkanen H, Heinonen IM, Torronen AR (2000) Eur Food Res Tech 212:75–80
41. Daniel EM, Krupnick AS, Heur YH, Blinzler JA, Nims RW, Stoner GD (1989) J Food Comp Anal 2:385–398
42. Goldberg DM, Hoffman B, Yang J, Soleas GJ (1999) J Agric Food Chem 47:3978–3985
43. Bobinaite R, Viskelis P, Venskutonis PR (2012) Food Chem 132: 1495–1501
44. Zhang J, Xiong Y, Peng B, Gao H, Zhou Z (2011) Comp Theo Chem 963:148–153
45. Teel RW, Babcock MS, Dixit R, Stoner GD (1986) Cell Biol Toxicol 2:53–62
46. Zhang Z, Hamilton SM, Stewart C, Strother A, Teel RW (1993) Anticancer Res 13:2341–2346
47. Wood AW, Huang MT, Chang RL, Newmark HL, Lehr RE, Yagi H, Sayer JM, Jerina DM, Conney AH (1982) Proc Natl Acad Sci USA 79:5513–5517
48. Hassoun EA, Walter AC, Alsharif NZ, Stohs SJ (1997) Toxicology 124:27–37
49. Priyadarsini KI, Khopde SM, Santosh SK, Mohan H (2002) J Agric Food Chem 50:2200–2206
50. Barch DH, Rundhaugen LM, Stoner GD, Pillay NS, Rosche WA (1996) Carcinogenesis 17:265–269
51. Muthenna P, Akileshwari C, Reddy GB (2012) J Biochem 442:221–230
52. Lee C, Yang W, Parr RG (1988) Phys Rev B 37:785–789
53. Becke AD (1993) J Chem Phys 98:5648–5652
54. Miertus S, Tomasi J (1982) Chem Phys 65:239–245
55. Miertus S, Scrocco E, Tomasi J (1981) Chem Phys 55:117–129
56. Woon DE, Dunning TH Jr (1993) J Chem Phys 98:1358–1371
57. Kendall RA, Dunning TH Jr, Harrison RJ (1992) J Chem Phys 96: 6796–6806
58. Perdew JP, Burke K, Wang Y (1996) Phys Rev B 54:16533–16539
59. Laidler KJ (2004) Chemical kinetics, 3rd edn. Pearson, Patparganj
60. Dennington R, Keith T, Millam J (2009) GaussView, version 5. Semichem, Shawnee Mission
61. Frisch MJ, Trucks GW, Schlegel HB, Scuseria GE, Robb MA, Cheeseman JR, Scalmani G, Barone V, Mennucci B, Petersson GA, Nakatsuji H, Caricato M, Li X, Hratchian HP, Izmaylov AF, Bloino J, Zheng G, Sonnenberg JL, Hada M, Ehara M, Toyota K, Fukuda R, Hasegawa J, Ishida M, Nakajima T, Honda Y, Kitao O, Nakai H, Vreven T, Montgomery JA Jr, Peralta JE, Ogliaro F, Bearpark M, Heyd JJ, Brothers E, Kudin KN, Staroverov VN, Kobayashi R, Normand J, Raghavachari K, Rendell A, Burant JC, Iyengar SS, Tomasi J, Cossi M, Rega N, Millam JM, Klene M, Knox JE, Cross JB, Bakken V, Adamo C, Jaramillo J, Gomperts R, Stratmann RE, Yazyev O, Austin AJ, Cammi R, Pomelli C, Ochterski JW, Martin RL, Morokuma K, Zakrzewski VG, Voth GA, Salvador P, Dannenberg JJ, Dapprich S, Daniels AD, Farkas O, Foresman JB, Ortiz JV, Cioslowski J, Fox DJ (2009) Gaussian 09, revision A1. Gaussian, Wallingford
62. Silva PJ, Ramos MJ (2011) Comp Theo Chem 966:120–126
63. Ess DH, Houk KN (2005) J Phys Chem A 109:9542–9553
64. Sousa SF, Fernandes PA, Ramos MJ (2007) J Phys Chem A 111: 10439–10452
65. Rossi M, Erlebacher J, Zacharias DE, Carrel HL, Iannucci B (1991) Carcinogenesis 12:2227–2232
66. Wright JS, Johnson ER, DiLabio GA (2001) J Am Chem Soc 123: 1173–1183